Solar Energy Vol. 41, No. 4, pp. 387–392, 1988
Printed in the U.S.A.

0038-092X/88 $3.00 + .00

An Opaque Cloud Cover Model of Sky Short Wavelength Radiance

A. W. HARRISON and C. A. COOMBES
Department of Physics, The University of Calgary, 2500 University Drive N.W., Calgary, Alberta, Canada, T2N 1I4N

Abstract—The average angular distribution of short wavelength sky radiance for clear, partly cloudy, and overcast sky conditions has been measured for the range of solar zenith angle 31° to 80°. Detailed analysis of this sky radiance data shows that the normalized sky radiance is given analytically by

$$N(\theta, \phi) = CN_0(\theta, \phi) + [1 - C]\, N_c(\theta, \phi)$$
$$\text{where} \quad N_0(\theta, \phi) = 0.45 + 0.12\,\theta^* + 0.43\cos\theta + 0.72e^{-1.88\psi}$$
$$N_c(\theta, \phi) = [1.63 + 53.7e^{-5.49\psi} + 2.04\cos^2\psi\cos\theta^*]\,[1 - e^{-0.19\mathrm{Sec}\theta}]\,[1 - e^{-0.53\mathrm{Sec}\theta^*}],$$

and θ^* is the solar zenith angle (radians), (θ, ϕ) is the sky radiance direction, ψ is the scattering angle (radians) between sky and sun directions, and C is the prevailing opaque cloud cover.

1. INTRODUCTION

Estimates of the solar short wavelength irradiance of sloping surfaces is important in solar energy utilization studies, building design work, and predictions of agricultural crop production. These estimates are usually based either on tilted surface irradiance models[1–5] or on models of the parent sky radiance[6–9]. In either case, models have to be validated, calibrated or both, to be of practical benefit to users and must be presented in terms of one or more readily available sky parameters. These parameters include the following: atmospheric turbidity (clear skies), solar zenith angle, direct solar beam transmittance, clearness index, fractional sunshine hours, cloud cover, and the like. Of these parameters, cloud cover is the most widely measured and is, therefore, an attractive parameter for use in any solar energy model calculations. The semiempirical model of sky short wavelength radiance presented here is based on cloud cover and solar zenith angle and follows two previous studies for completely clear and overcast skies respectively[10,11]. This model is referred to as the opaque cloud model (see following).

2. EXPERIMENTAL DATA BASE

The all-sky radiometer used to collect data for this study has been described in detail by Coombes and Harrison[12]. Only brief relevant details are given here. The instrument measures both direct solar and diffuse sky radiance in both short (0.3–3.0 μm) and long (3.0–80.0 μm) wavelength regions taking 12 min to complete an all-sky scan. Each scan is made at the same 95 equally spaced points over the hemispherical dome and is repeated once every 20 min. The long wavelength data are used to measure the prevailing opaque cover C_s according to the statistical technique described by Coombes and Harrison[13]. This study is based on radiometer data collected between July 1983 and March 1986 at a rural site in the Rocky Mountain foothills near Calgary, Alberta.

The short wavelength diffuse irradiance for each sky scan of a horizontal surface D was calculated from the corresponding measured sky radiance $N'_m(\theta, \phi)$ by proper integration over the sky dome. Sky radiance values in each sky scan were then converted to normalized values $N_m(\theta, \phi)$ according to

$$N_m(\theta, \phi) = \frac{\pi N'_m(\theta, \phi)}{D} \tag{1}$$

This process places all sky scans on the same relative radiance scale. ($N_m(\theta, \phi)$ would equal unity at all points in an isotropic sky.) Hence, each sky scan consisting of 95 values of $N_m(\theta, \phi)$ is characterized by one value of C_s, one value of D, and the value of solar zenith angle θ_s^* at which the sky scan occurred. All sky scans thus recorded were then divided into 66 sky-scan groups identified by the effective θ^* and C values indicated in Table 1. The number of sky scans in each group is n and the range of θ_s^* and C_s values corresponding to each effective θ^* and C value, respectively, are as follows: $\theta_s^* = 28°–35°$ ($\theta^* = 31°$); $\theta_s^* = 35°–45°$, ($\theta^* = 40°$); ... $\theta_s^* = 75°–85°$, ($\theta^* = 80°$); $C_s = 0.0–0.05$, ($C = 0.0$); $C_s = 0.05–0.15$, ($C = 0.1$); ... $C_s = 0.85–0.95$, ($C = 0.9$); $C_s = 0.95–1.0$, ($C = 1.0$). It should be noted that Calgary is at latitude 51°N so that the minimum observable θ_s^* value is 28°. The measured normalized radiances were averaged within each group at every one of the spatially distributed sky points (θ, ϕ) that is,

$$\bar{N}_m(\theta, \phi) = \frac{\Sigma N_m(\theta, \phi)}{n} \tag{2}$$

Contours of the resulting normalized sky radiance were then plotted using The University of Calgary Multics contour plotting routine for $\bar{N}_m(\theta, \phi) = 1.0, 2.0, 3.0,$

Table 1. Parameters relating to opaque cloud model of sky radiance.

0*	C	0.0	0.1	0.2	0.3	0.4	0.5	0.6	0.7	0.8	0.9	1.0
31°	n	71	115	149	54	57	21	33	32	36	43	64
	R	.833	.863	.938	.930	.900	.926	.935	.925	.930	.896	.969
40°	n	246	135	157	75	43	47	51	47	51	73	131
	R	.930	.925	.914	.939	.904	.926	.917	.953	.939	.960	.957
50°	n	565	141	71	56	63	55	50	52	79	104	254
	R	.893	.882	.903	.889	.890	.923	.922	.934	.961	.958	.983
60°	n	947	169	110	96	87	85	69	76	98	152	272
	R	.913	.939	.920	.912	.913	.851	.881	.893	.918	.960	.985
70°	n	1380	208	143	119	96	112	88	106	159	199	379
	R	.964	.961	.956	.945	.937	.888	.872	.886	.862	.955	.930
80°	n	1250	274	126	101	125	91	92	126	120	196	338
	R	.880	.871	.867	.860	.863	.859	.814	.905	.881	.891	.923

... and 1.0, 0.9, 0.8 .... The resulting 66 sky contour maps for $\theta^* = 31°, 40°, \ldots$ and $C = 0.0, 0.1, \ldots$ are shown in Fig. 1a, b, and c. Also shown in Fig. 2 is the larger-scale contour for $\theta^* = 70°$, $C = 0.1$ to indicate clearly the θ scale and order of normalized radiance values common to all contour maps in Fig. 1.

3. DISCUSSION

The sky radiance contour maps shown in Fig. 1 exhibit a definite pattern dependent on θ^* and C. Clear skies ($C = 0.0$) and low sun ($\theta^* = 80°$) have the highest degree of anisotropy ($\bar{N}_m(\theta, \phi) = \sim 0.3$ minimum to > 20.0 maximum), whereas overcast skies ($C = 1.0$) and high sun ($\theta^* = 31°$) are most nearly isotropic, ($\bar{N}_m(\theta, \phi) = \sim 0.6$ minimum to ~ 1.3 maximum). The regularity with which the pattern changes with cloud cover and sun position suggests the possibility of being able to respresent sky radiance analytically with C and θ^* as sky parameters. Previous studies of completely clear and completely overcast skies[10,11] have shown that the corresponding normalized sky radiances can be adequately represented by the analytical expressions, respectively,

$$N_c(\theta, \phi) = [1.63 + 53.7e^{-5.49\psi} + 2.04 \cos^2 \psi \cos \theta^*][1 - e^{-0.19\mathrm{Sec}\theta}][1 - e^{-0.53\mathrm{Sec}\theta^*}] \quad (3)$$

and

$$N_0(\theta, \phi) = 0.45 + 0.12\theta^* + 0.43 \cos \theta + 0.72e^{-1.88\psi} \quad (4)$$

where $\cos \psi = \cos \theta^* \cos \theta + \sin \theta^* \sin \theta \cos \phi$ and θ^* is in radians. It is reasonable to suppose that the normalized sky radiance of a partly cloudy sky would be just the weighted sum of clear and overcast radiances:

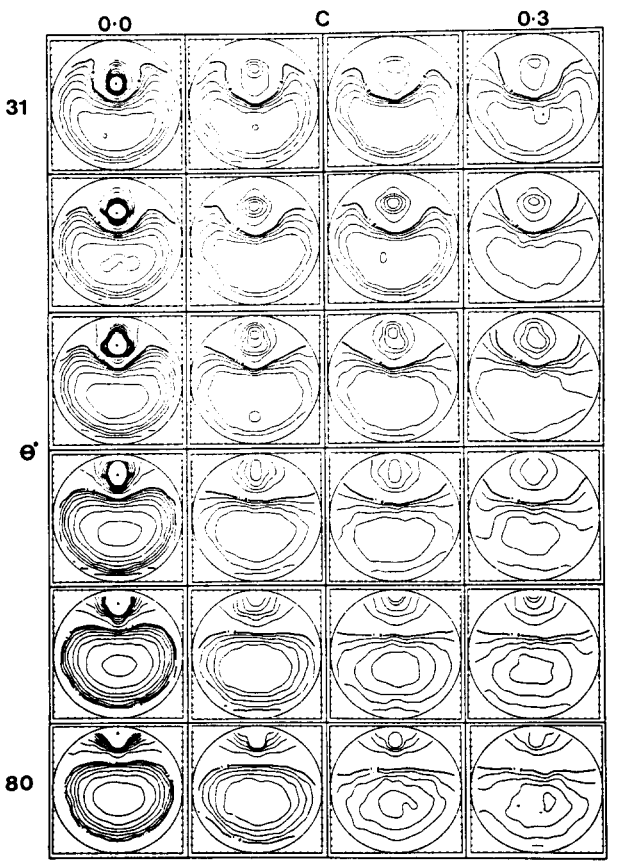

Fig. 1a. Measured sky radiance contour maps for $\theta^* = 31°, 40°, \ldots 80°$ and $C = 0.0, 0.1, 0.2$, and 0.3.

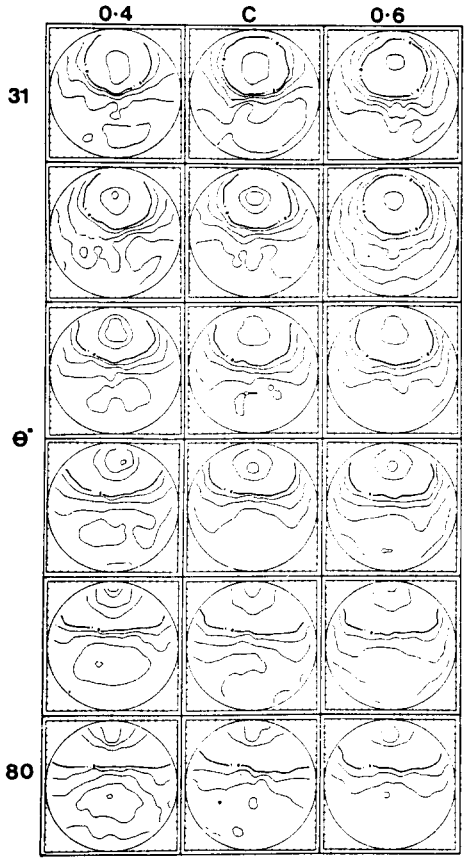

Fig. 1b. Measured sky radiance contour maps for $\theta^* = 31°, 40°, \ldots 80°$ and $C = 0.4, 0.5$, and 0.6.

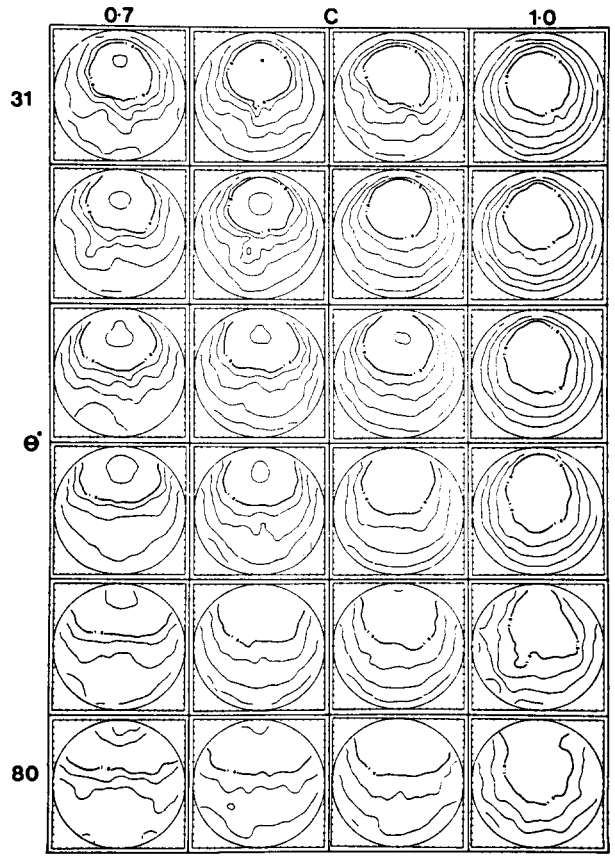

Fig. 1c. Measured sky radiance contour maps for θ^* 31°, 40°, ... 80° and $C = 0.7, 0.8, 0.9$, and 1.0.

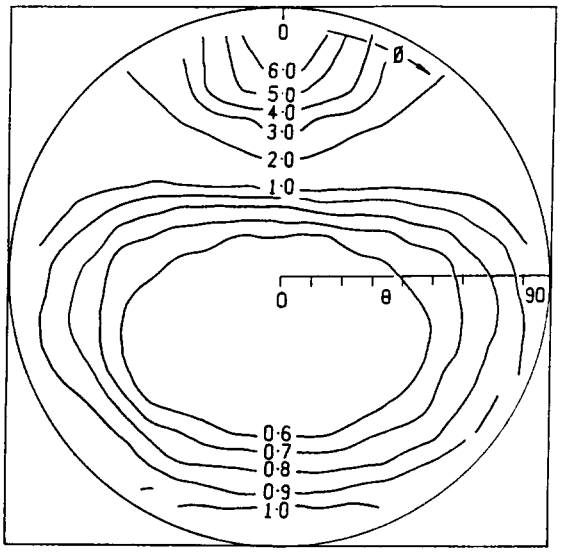

Fig. 2. Measured sky radiance contour map for $\theta^* = 70°$ and $C = 0.1$.

$$N(\theta, \phi) = CN_0(\theta, \phi) + [1 + C]\, N_c(\theta, \phi) \quad (5)$$

This supposition was tested by comparing $\bar{N}_m(\theta, \phi)$ with $N(\theta, \phi)$ calculated from (5) for each (θ^*, C) data set by calculating the simple product moment correlation coefficient R. The results of these calculations are given in Table 1. Application of Student's t test showed that for all 66 data sets the chance of obtaining the calculated value of R for a true value of $R = 0$ is <0.1%. In general, the values of R in Table 1 are relatively high indicating that, eqn (5) represents the true sky radiance very well. The lowest values of R occur for partly cloudy skies as might be expected. In the range $C = 0.3$ to 0.8 the best value of R (.961) occurs for $\theta^* = 50°$, $C = 0.8$, and the worst value of R (.814) occurs for $\theta^* = 80°$, $C = 0.6$. Corresponding measured and calculated normalized radiance contours are shown in Figs. 3 and 4, respectively. The associated measured and calculated sky radiance values are shown in Figs. 5 and 6. Even for the worst case, the agreement between

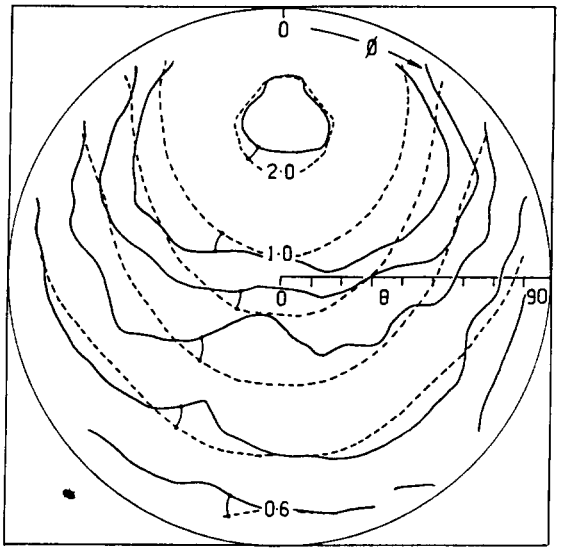

Fig. 3. Contours of $\bar{N}_m(\theta, \phi)$ solid line, and $N(\theta, \phi)$ dashed line for $\theta^* = 50°$ and $C = 0.8$.

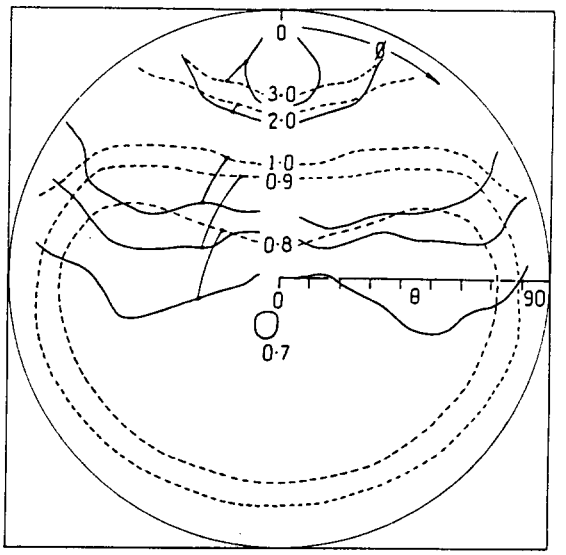

Fig. 4. Contours of $\bar{N}_m(\theta, \phi)$ solid line, and $N(\theta, \phi)$ dashed line for $\theta^* = 80°$ and $C = 0.6$.

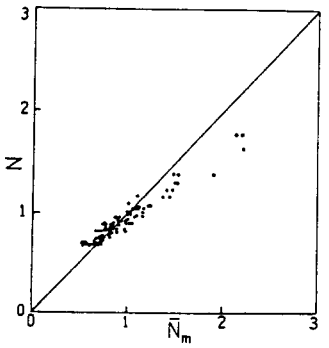

Fig. 5. Comparison of measured $\bar{N}_m(\theta, \phi)$ and calculated $N(\theta, \phi)$ sky radiances for the 95 equally spaced sky positions with $\theta^* = 50°$, $C = 0.8$.

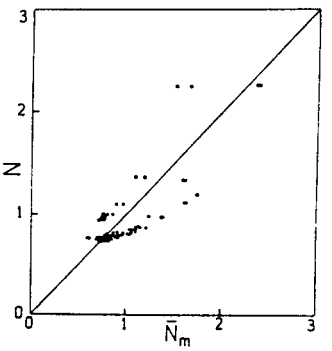

Fig. 6. Comparison of measured $\bar{N}_m(\theta, \phi)$ and calculated $N(\theta, \phi)$ sky radiances for the 95 equally spaced sky positions with $\theta^* = 80°$, $C = 0.6$.

$\bar{N}_m(\theta, \phi)$ and $N(\theta, \phi)$ must be considered at least satisfactory considering the difficulty of fitting a single expression (5) to any cloud cover or sun position.

4. CONCLUSION

This study has shown that the single analytical expression (5) can be used to estimate the short wavelength *normalized* sky radiance using only opaque cloud cover and solar zenith angle as sky parameters. To obtain an estimate of the *absolute* sky radiance, the prevailing short wavelength diffuse irradiance of a horizontal surface is also required,

$$N'(\theta, \phi) = \frac{DN(\theta, \phi)}{\pi} \tag{6}$$

NOMENCLATURE

- ψ scattering angle between sky and sun directions
- θ sky zenith angle
- ϕ sky azimuth angle relative to sun
- $N'_m(\theta, \phi)$ measured sky shortwave radiance
- $N_m(\theta, \phi)$ measured normalized sky shortwave radiance
- $\bar{N}_m(\theta, \phi)$ average measured normalized sky shortwave radiance
- $N'(\theta, \phi)$ opaque cloud model absolute sky shortwave radiance
- $N(\theta, \phi)$ opaque cloud model normalized sky shortwave radiance
- $N_c(\theta, \phi)$ empirical model normalized *clear* sky shortwave radiance
- $N_0(\theta, \phi)$ empirical model normalized *overcast* sky shortwave radiance
- C_i opaque cloud cover corresponding to each sky scan
- C effective opaque cloud cover corresponding to each group of sky scans
- n number of all sky scans averaged for each (θ^*, C) group
- D shortwave diffuse irradiance of a horizontal surface
- θ_i^* solar zenith angle of each sky scan
- θ^* effective solar zenith angle for each group of sky scans
- R simple product moment correlation coefficient

Acknowledgments—The authors wish to thank the Natural Sciences and Engineering Research Council for their generous financial support of this project. Appreciation is also due to Mrs. W. Ma for undertaking the necessary computer analysis of data.

REFERENCES

1. J. E. Hay, Study of shortwave radiation on non-horizontal surfaces. Rep. 79-12, Atmospheric Environment Service, Downsview, Ontario (1979).
2. J. E. Hay, Calculation of monthly mean solar radiation for horizontal and inclined surfaces. *Solar Energy* **23**, 301, (1979).
3. T. M. Klucher, Evaluation of models to predict insolation on tilted surfaces. *Solar Energy* **23**, 111, (1979).
4. S. K. Klein, Calculation of monthly average insolation on tilted surfaces. *Solar Energy* **19**, 253 (1977).
5. C. Gueymard, An anisotropic solar irradiance model for tilted surfaces and its comparison with selected engineering algorithms. *Solar Energy* **38**, 367, (1987).
6. M. D. Steven, Standard distributions of clear sky radiance. *Quart. J. R. Met. Soc.* **103**, 457, (1977).
7. F. C. Hooper, A. P. Brunger, and C. S. Chan, A clear sky model of diffuse sky radiance. *J. Solar Energy Eng., (Trans. A.S.M.E.)* **109**, 9, (1987).
8. R. Perez, R. Stewart, C. Arbogast, R. Seals, and J. Scott, An anisotropic hourly diffuse radiation model for sloping surfaces: Description performance, validation, site dependency evaluation. *Solar Energy* **36**, 481, (1986).
9. C. Gueymard, Une paramétrisation de la luminance énergétique du ciel clair en fonction de la turbidite. *Atmosphere-Ocean* **24**, 1, (1986).
10. A. W. Harrison and C. A. Coombes, Angular distribution of clear sky short wavelength radiance. *Solar Energy* **40**, (1), 57, (1988).
11. C. A. Coombes and A. W. Harrison, Angular distribution of overcast sky short wavelength radiance. *Solar Energy* (accepted for publication 1988).
12. C. A Coombes and A. W. Harrison, An automatic all sky scanning radiometer. *Can. J. Phys.* **60**, 919, (1982).
13. C. A. Coombes and A. W. Harrison, Radiometer estimation of cloud cover. *J. Atmos. Oceanic Tech.* **2**, (4), 482, (1985).